ELSEVIER

Surface Science 486 (2001) L507–L512

SURFACE SCIENCE

www.elsevier.nl/locate/susc

Surface Science Letters

Electron transport on a single CdS nanocrystal formed on self-assembled monolayer at room temperature

Peng Jiang [a,*], Zhong-Fan Liu [b], Sheng-Min Cai [b]

[a] *Beijing Laboratory of Vacuum Physics, Institute of Physics and Center for Condensed Matter Physics, Chinese Academy of Sciences, P.O. Box 2724, Beijing 100080, China*

[b] *Center for Nanoscale Science and Technology (CNST) and College of Chemistry and Molecular Engineering, Peking University, Beijing 100871, China*

Received 6 December 2000; accepted for publication 28 March 2001

Abstract

Electron transport through a single CdS nanocrystal with the size of 2 nm was investigated using scanning tunneling microscope (STM) at room temperature in air. The nanocrystal was prepared by the exposure of 11-mercaptoundecanoic acid self-assembled monolayer adsorbed bivalent metal ions on Au(1 1 1) substrate to an H_2S atmosphere. STM was employed to image, to position an individual CdS nanoparticle, and finally to detect its current–voltage (I–V) characteristics. The results demonstrated clear Coulomb blockade and Coulomb staircase effects in the I–V curves. Furthermore, by varying the distance between STM tip and CdS nanoparticle, we also found the dependence of staircase width on the air gap in the local I–V characteristics, which can be well explained in terms of semi-classical double-barrier tunneling model. © 2001 Elsevier Science B.V. All rights resrved.

Keywords: Tunneling; Scanning tunneling microscopy; Self-assembly; Cadmium sulphide

Single-electron tunneling (SET), taking place in quantum-confined low-dimensional systems, has attracted extreme interest of researchers. It has been recognized as the potential fundament for future single-electron devices [1–3]. In recent few years, the effect has been verified in many nanometer structures [4–13]. Among them, a typical structure is that a small metal or semiconductor nanoparticle is sandwiched between two external metal electrodes through two tunneling junctions. In such system, if the total capacitance C of the center nanoparticle to its environment is small enough to make the single-electron charging energy ($e^2/2C$) exceed thermal energy kT, then, thermal fluctuation will not smear the charging effect, and SET phenomena (or Coulomb blockade and staircases) can be observed. In general, at room temperature, investigation of the SET behavior requires the size of center electrode to be reduced down to below 10 nm to meet the condition ($e^2/2C > kT \approx 26$ meV). While, from the view of application, an inevitable fact is that the devices must be operated at room temperature. Therefore, the new construction of ultrasmall double-barrier tunneling junction (DBTJ) systems for the objective of future devices has become more and more interesting.

* Corresponding author. Tel./fax: +86-10-62556598.
E-mail address: pjiang@aphy.iphy.ac.cn (P. Jiang).

PII: S0039-6028(01)01093-7

The question followed is how to characterize such small particles and utilize them as center mesoscopic island. Advent of scanning tunneling microscope (STM) helps us to solve the dilemma. STM has proven to be versatile as a tool to image, and to localize on single nanoparticle to detect its local electronic properties. Up to now, many groups have employed it to measure electronic properties of nanocrystals tethered on various substrates, striking results have also been achieved under low [14–18] and room temperature [19–24] conditions. In the present paper, we describe a strategy for growing CdS nanoparticles on gold (Au) (1 1 1) substrate modified by 11-mercaptoundecanoic acid self-assembled monolayer (SAM), then employ STM tip to see and to position a single CdS nanoparticle to construct DBTJ system, in which the CdS nanoparticle is served as center island while air and organic monolayer as two tunneling junctions, for systematic SET studies at room temperature.

The preparation method of the extremely small CdS nanoparticles is similar to one suggested by Fendler and co-workers [25], except the replacement of LB membranes by SAM on a Au(1 1 1) substrate. The Au(1 1 1) substrate was obtained by melting a 0.5 mm diameter Au wire in hydrogen–oxygen flame and sequentially quenching in ultrapure water. The process gave a single crystal bead with several Au(1 1 1) facets (see Fig. 1). Thus-prepared substrate was then immersed into the $\sim 10^{-3}$ mol/l ethanol solution containing 11-mercaptoundecanoic acid for forming a layer of SAM, followed by adsorbing cadmium ions (Cd^{2+}) in 10^{-4} mol/l $CdCl_2$ solution, and finally exposed to H_2S gas to form CdS nanoparticles on it.

STM imaging was performed on the sample in constant current mode. Fig. 2(a) shows a typical STM image of the CdS nanoparticles nucleated on an Au(1 1 1) surface through SAM coupling layer. The sizes of the nanoparticles can be estimated through lateral section analysis, which gives the mean diameter of 2.1 ± 0.3 nm averaged from 100 CdS nanoparticles. The experimental result indicates that the SAM can effectively nucleate CdS nanocrystals with narrow size distribution. Thus-synthesized nanocrystals are very suitable to serve as center Coulomb island for room temperature

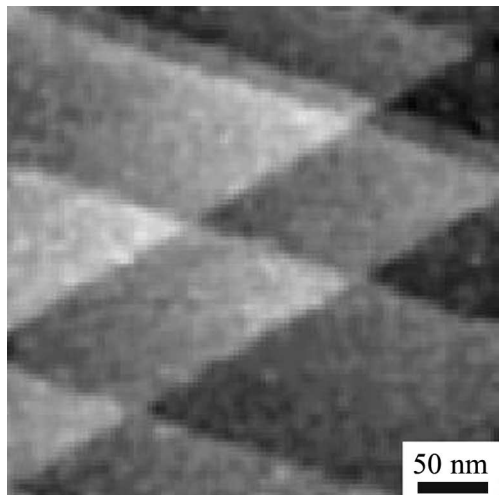

Fig. 1. A typical STM image of a Au(1 1 1) facet revealing wide (1 1 1) terraces separated by the monoatomic step lines intersecting at an angle of 60° or 120°.

SET investigation. To further provide the direct proof of formation of the CdS nanoparticles, we also synthesized CdS nanoparticles on STM gold-tip apex prepared by electrochemical etching method. The modified Au tips were directly used for the TEM observations. Fig. 2(b) presents the typical TEM image in the tip apex region, from which a single CdS nanoparticle was obviously found. It can be obtained from the image that the lattice constant between the planes is 0.31 nm, considerably agreed with that of wurtzite CdS-(1 0 1) ($d = 0.3160$ nm). Its size approaches 2 nm in diameter, which accounts for the result obtained by STM characterization.

For the measurements of current–voltage (I–V) characteristics of a single nanoparticle, we firstly imaged the CdS nanoparticles, and located STM gold tip over a chosen $\sim$2 nm CdS nanoparticle (see Fig. 3), finally switched off feedback to detect its I–V characteristics at certain tunnel current setpoint and fixed bias voltage. With continuous increase of the applied voltage, we found that the small DBTJ system was firstly charged and the current flowing through the system approached zero, which implies that the current is blocked. When the voltage went beyond certain threshold, electrons started to cross the island (see Fig. 4). Further, the long-term scanning stability of the

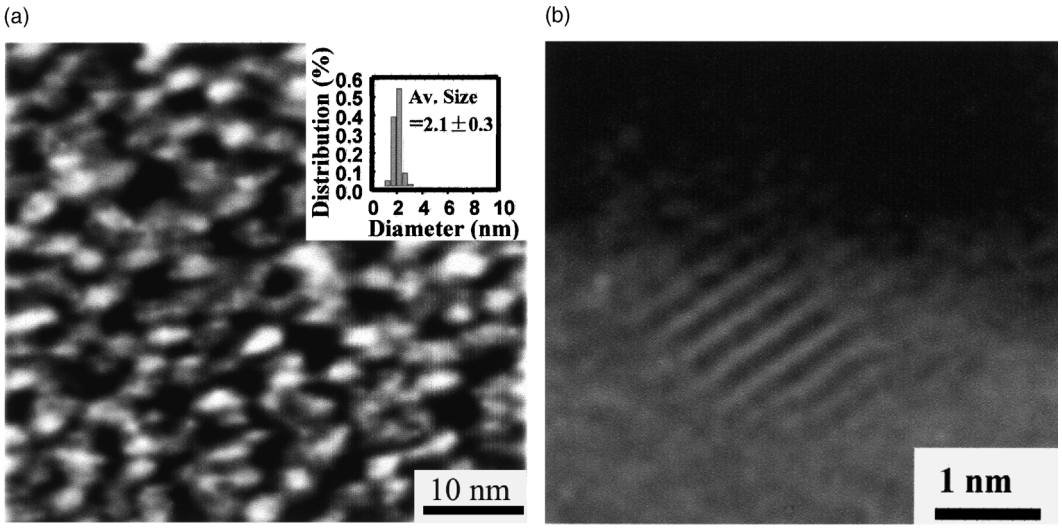

Fig. 2. (a) Constant current mode STM image of CdS nanoparticles formed on Au(1 1 1) surface modified by 11-mercaptoundecanoic acid. (b) A high resolution TEM micrograph of a single CdS nanoparticle on Au tip apex.

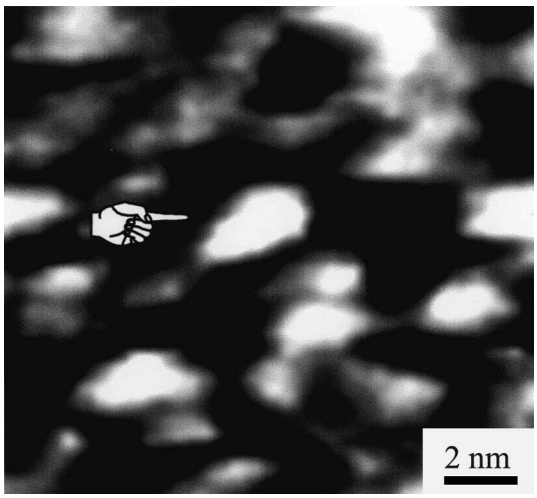

Fig. 3. Constant current mode STM image of a chosen ~2 nm CdS nanoparticle on Au(1 1 1) substrate.

sample allowed us to measure a series of I–V characteristics with the respect to the z displacement of tip. Typical data are shown as a function of the tunnel current setpoint in Fig. 4. Clear Coulomb blockade and staircases were observed in the I–V curves. For clarity, the corresponding $\mathrm{d}I/\mathrm{d}V$ vs. V curves were also plotted in Fig. 4, which shows a series of equi-distant peaks. It is worth noting that the staircase width of voltage strongly depends on the setpoint current, varying from 320 to 180 mV when setpoint current is increased from 1 to 4 nA. The result is extremely consistent with our previous report [23] where single CdS nanoparticle was tethered on STM tip. The electrostatic charging energy of the system estimated from the stepwidth of voltage apparently changes from 160 to 90 meV, each far higher than thermal fluctuation energy at room temperature (~26 meV). The corresponding tunneling capacitance C_Σ changes from 5.0×10^{-19} to 8.9×10^{-19} F with the variation of setpoint from 1 to 4 nA, each being of the same order ($C \sim 9.9 \times 10^{-19}$ F, $C = 4\pi r \varepsilon_0 \varepsilon_r$, $\varepsilon_{r(CdS)} = 8.9$) as that estimated on the basis of a 2.0 nm sized spherical CdS nanoparticle. In addition, asymmetric shapes at positive and negative bias voltages have also been found in I–V curves, suggesting a non-zero value of the fraction charge Q_0 existing on the CdS nanoparticle. In another aspect, some wider undistinguished peaks in $\mathrm{d}I/\mathrm{d}V$–V dependences hint the existence of additional substructure smeared by higher temperature.

In order to explain the observed phenomena, a simplified double-barrier tunneling model can be applied. The air gap between STM tip and CdS

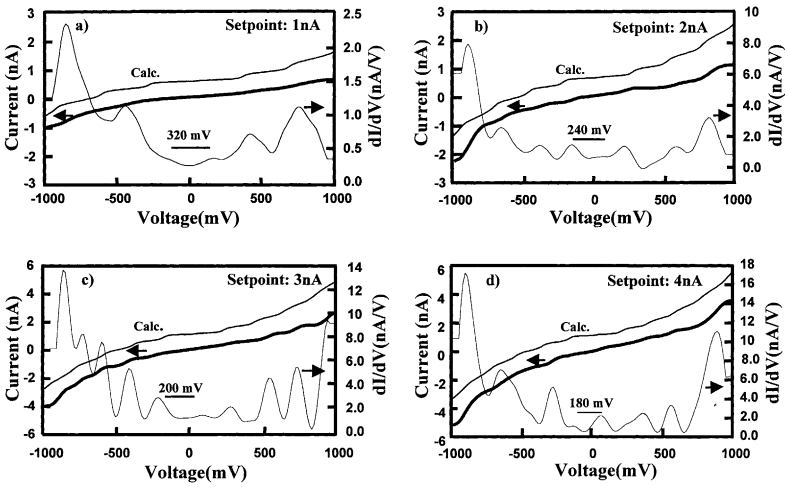

Fig. 4. The I–V characteristics (thick solid lines) obtained at various setpoint current and fixed bias voltage on a chosen CdS nanoparticle at room temperature in air, clear Coulomb blockade and staircases occur. The fitting curves (thin solid lines) represent theoretical curves obtained by the globe minimum in the mean square deviation fitting in terms of semi-classical tunneling theory. The junction parameters for various setpoint currents are: (a) $C_1 = 4.9 \times 10^{-19}$ F, $C_2 = 2.5 \times 10^{-19}$ F, $R_1 = 2.0$ GΩ, $R_2 = 23$ MΩ, $Q_0 = 0.0e$, $\alpha = 1$. (b) $C_1 = 6.8 \times 10^{-19}$ F, $C_2 = 2.5 \times 10^{-19}$ F, $R_1 = 800$ MΩ, $R_2 = 23$ MΩ, $Q_0 = -0.2e$, $\alpha = 1$. (c) $C_1 = 8.0 \times 10^{-19}$ F, $C_2 = 2.5 \times 10^{-19}$ F, $R_1 = 410$ MΩ, $R_2 = 23$ MΩ, $Q_0 = -0.4e$, $\alpha = 1$. (d) $C_1 = 8.9 \times 10^{-19}$ F, $C_2 = 2.5 \times 10^{-19}$ F, $R_1 = 320$ MΩ, $R_2 = 23$ MΩ, $Q_0 = -0.2e$, $\alpha = 1$, and $T = 298$ K.

nanoparticle is assigned as the first junction and 11-mercaptoundecanoic acid monolayer between CdS nanoparticle and Au(1 1 1) substrate as the second junction. We assume that each junction has a capacitance, an effective resistance and a tunneling rate associated with it, denoted by C_i, R_i, and Γ_i, $i = 1,2$. In such double-barrier system model, we find that when varying the locked tunnel current setpoint at fixed bias voltage, the asymmetry of the structure can be change. We think that in this case, the second barrier should reasonably keep fixed whereas the first, air junction, can be adjusted by the change of vertical position of the tip. Therefore, increasing setpoint current is in fact to move the tip towards the CdS island so that reduce the distance between tip and CdS nanoparticle. This can make C_1 become large. As a result, the width of Coulomb blockade ($\Delta V = e/C_\Sigma$) becomes narrow and the number of staircase grows, indicating the increase of number of excess electrons on the island.

According to the discussion mentioned above, a computer program was developed in terms of the semi-classical double tunneling model [26–28]. The numerical calculation simulation provides the theoretical fitting curves (see Fig. 4). In order to account for the non-linear background and asymmetric nature in the experimental I–V curves, in fitting procedure, we set a bias dependent resistance $R(V) = R_0/(1 + \alpha V^2)$ [29] into the tunneling rate Γ at the double tunneling junctions and a fractional charge Q_0 which may exist on the CdS nanoparticle. As a result, in Fig. 4, the fitting I–V curves well match the experimental curves. For clearly determining the rationality of variation of the junction parameters with the vertical shift of the tip, the tunneling resistance R_i, and capacitance C_i in Fig. 4 are plotted in Fig. 5 as a function of the setpoint current. It can be seen in Fig. 5 that a rapid decrease in R_1 and a slightly increase in C_1 occur as the separation between tip and CdS nanoparticle decreases, at the same time, the resistance R_2 and capacitance C_2 between the CdS island and Au substrate remain fixed as the setpoint current changes. The ratio of R_1C_1/R_2C_2 estimated from the fitting parameters is found to fall in the range between 49 and 169, suggesting the highly asymmetry of the two tunneling junc-

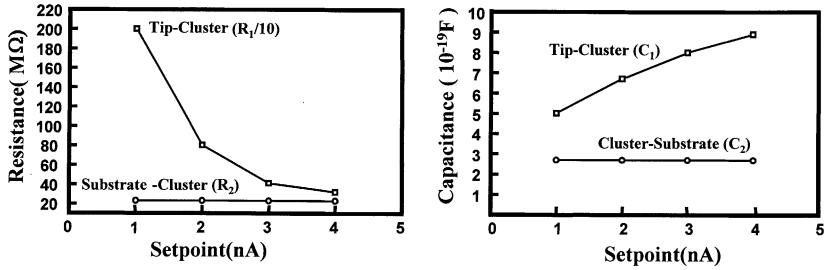

Fig. 5. Plot of fitting parameters vs. setpoint current used for the *I–V* measurements shown in Fig. 4.

tions, which can be regarded as the origin of the appearance of Coulomb staircases.

In conclusion, we present an approach to fabricating ultrasmall DBTJs by combining self-assembly and STM techniques. In such architecture, CdS nanoparticle serves as center Coulomb island and air and organic monolayer as tunneling junctions. Clear Coulomb blockade and staircases have been observed in the system by empolying STM at room temperature. Moreover, we have also observed the vertical position dependent *I–V* characteristics on the chosen CdS nanoparticle. The phenomena can be well described by semi-classical double-barrier tunneling theory. Next step, the study of horizontal position *I–V* dependence of a CdS nanoparticle will be performed, which is also very important aspect for constructing nanometer electronic devices.

Acknowledgements

The authors thank Professor Reifenberger of Purdue University in USA for kind help on the programming of theoretical calculation. The work has been financially supported by the National Nature Science Foundation of China (NSFC).

References

[1] H. Grabert, M.H. Devoret, Single charge tunneling, Coulomb Blockade Phenomena in Nanostructure, NATO ASI Series B, vol. 294, Plenum, New York, 1992.
[2] D.K. Ferry, H.L. Grubin, C. Jacoboni, A.P. Jauho, Quantum Transport in Ultrasmall Devices, NATO ASI Series B, vol. 342, Plenum, New York, 1994.
[3] M.A. Kastner, Nature 389 (1997) 667.
[4] R.P. Andres, T. Bein, M. Dorogi, S. Feng, J.I. Henderson, C.P. Kubiak, W. Mahoney, R.G. Osifchin, R. Reifenberger, Science 272 (1996) 1323.
[5] D.L. Klein, P.L. McEuen, J.E.B. Katari, R. Roth, A.P. Alivisatos, Appl. Phys. Lett 68 (1996) 2574.
[6] D.L. Klein, R. Roth, A.K.L. Lim, A.P. Alivisatos, P.L. McEuen, Nature 389 (1996) 699.
[7] D.L. Feldheim, K.C. Grabar, M.J. Natan, T.E. Mallouk, J. Am. Chem. Soc. 118 (1996) 7640.
[8] R.S. Ingram, M.J. Hostetler, R.W. Murry, T.G. Schaaff, T.J. Khoury, R.L. Whetten, T.P. Bigioni, D.K. Guthrie, P.N. First, J. Am. Chem. Soc. 119 (1997) 9279.
[9] L.C. Grousseau, Q. Zhao, D.A. Shultz, D.L. Feldheim, J. Am. Chem. Soc. 120 (1998) 7645.
[10] U.-W. Grummt, M. Geissler, T. Drechsler, H. Fuchs, R. Staub, Angew. Chem. Int. Ed. 37 (1998) 3286.
[11] E.M. Ford, H. Ahmed, Appl. Phys. Lett. 75 (1999) 421.
[12] M. Bockrath, D.H. Cobden, P.L. McEuen, N.G. Chopra, A. Zettl, A. Thess, R.E. Smalley, Science 275 (1997) 1922.
[13] D. Porath, O. Millo, J. Appl. Phys. 81 (1997) 2241.
[14] T.A. Fulton, G.J. Dolan, Phys. Rev. Lett. 59 (1987) 109.
[15] P.J.M. van Bentum, H. van Kempen, L.E.C. van de Leemput, P.A.A. Teunissen, Phys. Rev. Lett. 60 (1988) 369.
[16] P.J.M. van Bentum, R.T.M. Smokers, H. van Kempen, Phys. Rev. Lett. 60 (1988) 2543.
[17] C. Schönenberger, H. van Kempen, J.M. Kerkhorf, H.C. Donkersloot, Appl. Surf. Sci. 67 (1993) 222.
[18] C. Schönenberger, H. van Houten, Physica B 189 (1993) 218.
[19] P. Facci, V. Erokhin, S. Carrara, C. Nicolini, Proc. Natl. Acad. Sci. 93 (1996) 10556.
[20] V. Erokhin, P. Facci, S. Carrara, C. Nicolini, Thin Solid Films 284 (1996) 891.
[21] U. Simon, Adv. Mater. 10 (1998) 1487.
[22] K.H. Park, M. Shin, J.S. Ha, W.S. Yun, Y.J. Ko, Appl. Phys. Lett. 75 (1999) 139.
[23] P. Jiang, Z.F. Liu, S.M. Cai, Appl. Phys. Lett. 75 (1999) 3023.
[24] A. Taleb, F. Silly, A.O. Gusev, F. Charra, M.P. Pileni, Adv. Mater. 12 (2000) 633.
[25] J.H. Fendler, F.C. Meldrum, Adv. Mater. 7 (1995) 607.

[26] A.E. Hanna, M. Tinkham, Phys. Rev. B. 44 (1991) 5919.
[27] M. Amman, R. Wilkins, E. Ben-Jacob, P.D. Maker, R.C. Jaklevic, Phys. Rev. B 43 (1991) 1146.
[28] K. Mullen, E. Ben-Jacob, R.C. Jaklevic, Z. Schuss, Phys. Rev. B 37 (1998) 98.
[29] K.H. Park, J.S. Ha, W.S. Yun, M. Shin, K.W. Park, E.H. Lee, Appl. Phys. Lett. 71 (1997) 1469.